Protein-Induced Formation of Cholesterol-Rich Domains[†]

Richard M. Epand,*[,‡] Shohei Maekawa,[§] Christopher M. Yip,[||] and Raquel F. Epand[‡]

Department of Biochemistry, McMaster University, Hamilton, Ontario, Canada L8N 3Z5, Department of Bioinformation, Division of Bioscience, Graduate School of Science and Technology, Kobe University, Nada-ku, Rokkohdai, Kobe 657-8501, Japan, and Department of Chemical Engineering and Applied Chemistry, Institute of Biomaterials and Biomedical Engineering, University of Toronto, Toronto, Ontario, Canada M5S 3G9

Received May 2, 2001; Revised Manuscript Received July 5, 2001

ABSTRACT: A major protein of neuronal rafts, NAP-22, binds specifically to cholesterol. We demonstrate by circular dichroism that NAP-22 contains a significant amount of β-structure that is not sensitive to binding of the protein to membranes, suggesting that a major portion of the protein does not insert deeply into the membrane. The free energy of binding of NAP-22 to liposomes of dioleoylphosphatidylcholine with 40% cholesterol is -7.3 ± 0.5 kcal/mol. NAP-22 mixed with dipalmitoylphosphatidylcholine and 40% cholesterol partitions into the detergent insoluble fraction in the presence of 1% Triton X-100. NAP-22 also causes this insoluble fraction to become enriched in cholesterol relative to phospholipid, again demonstrating the ability of this protein to segregate cholesterol and phospholipids into domains. Differential scanning calorimetry results demonstrate that NAP-22 promotes domain formation in liposomes composed of cholesterol and phosphatidylcholine. This is shown by NAP-22-promoted changes in the shape and enthalpy of the phase transition of phosphatidylcholine as well as by the appearance of cholesterol crystallite transitions in membranes composed of phosphatidylcholine with either saturated or unsaturated acyl chains. In situ atomic force microscopy revealed a marked change in the surface morphology of a supported bilayer of dioleoylphosphatidylcholine with 0.4 mole fraction of cholesterol upon addition of NAP-22. Prior to the addition of the protein, the bilayer appears to be a molecularly smooth structure with uniform thickness. Addition of NAP-22 resulted in the rapid formation of localized raised bilayer domains. Remarkably, there was no gross disruption or erosion of the bilayer but rather simply an apparent rearrangement of the lipid bilayer structure due to the interaction of NAP-22 with the lipid. Our results demonstrate that NAP-22 can induce the formation of cholesterol-rich domains in membranes. This is likely to be relevant in neuronal membrane domains that are rich in NAP-22.

A growing body of evidence shows that cholesterol-rich domains are present in the membranes of many mammalian cells. They have been the subject of much recent attention because of their importance in certain signal transduction pathways (*1*−*3*). These domains typically exhibit low fluidity (*4*) and are rich in lipids such as sphingomyelin or glycosphingolipids that melt at high temperatures (*5*, *6*). These domains, known as "rafts", are believed to be in a unique physical state, termed the liquid-ordered or L_o phase. This phase is characterized by lipid having extended acyl chains, like the gel phase, but rapid lateral mobility, like the liquid crystalline phase. It is thought that sphingomyelin, because of its high transition temperature, abundance of saturated acyl chains, and tendency to associate with cholesterol, is necessary for the formation of these raft structures (*5*). Rafts are transient in nature and have been observed directly only by single-particle tracking (*7*, *8*) or by photonic force microscopy (*8*, *9*). Cholesterol-rich domains are also found in morphologically distinct structures within the plasma membrane termed caveoli (*10*).

NAP-22, a myristoylated protein localized to the synapse (*11*), is a major component of the detergent insoluble, low-density fraction from rat brain. Unlike typical rafts discussed above, the detergent insoluble fraction from neurons is relatively low in sphingomyelin content but yet rich in cholesterol (*12*). The fact that NAP-22 is myristoylated is likely to be important for its ability to sequester to cholesterol-rich domains (*13*). A protein with a high degree of sequence homology and likely with very similar properties, CAP-23, was first identified by Widmer and Caroni (*14*). Along with GAP-43 and MARCKS, CAP-23 is thought to regulate cell cortex actin dynamics (*15*). NAP-22 is enriched in the growth cone, a specialized neurological structure present at the tip of an extended neurite (*16*), and is thought to share a unique role with GAP-43 in neurite outgrowth and anatomical plasticity (*17*). The shared roles of GAP-43 and NAP-22 are indicated by the observation that GAP-43 can replace the function of NAP-22 in knockout mice (*17*). Coexpression of GAP-43 and CAP-23 can promote a 60-fold increase in the level of regeneration of doral root ganglion axons in adult mice after spinal cord injury in vivo (*18*).

[†] This work was supported by Grant MT-7654 from the Canadian Institute of Health Research.

* To whom correspondence should be addressed: Department of Biochemistry, McMaster University, Hamilton, Ontario, Canada L8N 3Z5. E-mail: epand@mcmaster.ca. Fax: (905) 521-1397. Telephone: (905) 525-9140, ext. 22073.

[‡] McMaster University.

[§] Kobe University.

[||] University of Toronto.

10.1021/bi010897s CCC: $20.00
Published on Web 08/11/2001

It has been reported that NAP-22 binds specifically in vitro only to cholesterol-containing liposomes (*12*). It is also known that in addition to binding to membranes, NAP-22 binds to calmodulin (*16*), but without an accompanying conformational change in its calmodulin-binding domain (*19*). Moreover, this protein has been shown to be particularly resistant to denaturation (*16*). In this work, we study the conformational and cholesterol binding properties of NAP-22 and, in particular, investigate whether the specificity for cholesterol binding is sufficient to induce the formation of cholesterol-rich domains in membranes.

MATERIALS AND METHODS

Materials. NAP-22 was isolated from the brains of 2-week-old rats, as previously described (*12*). Phospholipids were purchased from Avanti Polar Lipids (Alabaster, AL). Cholesterol was purchased from Northern Lipids (Vancouver, BC) and [7-^{3}H(N)]cholesterol from American Radiolabeled Chemicals (St. Louis, MO).

Circular Dichroism (CD). The CD spectra were recorded using an AVIV model 61 DS CD instrument (AVIV Associates, Lakewood, NJ). The sample was contained in a 1 mm path length cell that was maintained at 37 °C in a thermostated cell holder. The CD data are expressed as the mean residue ellipticity. The secondary structure was estimated using a neural network-based algorithm (*20*) as well as by the curve-fitting procedure of Yang et al. (*21*). All CD runs were made with protein dissolved in 10 mM sodium phosphate buffer containing 0.15 M NaF and 1 mM EDTA (pH 7.4). Protein concentrations were determined using a BCA protein assay.

Incorporation of NAP-22 into Multilamellar Vesicles (MLV).[1] NAP-22 was incorporated into the membrane by hydrating lipid films with a solution of the protein in 10 mM Tris-HCl, 150 mM NaCl, 2 mM $MgCl_2$, 0.2 mM EGTA, and 1 mM dithiothreitol (pH 7.5). The final protein concentration was ~7 μM and that of the lipid 3.5 mM. The lipids that were used were 1-stearoyl-2-oleoylphosphatidylcholine (SOPC), dioleoylphosphatidylcholine (DOPC), dipalmitoylphosphatidylcholine (DPPC), or 1-stearoyl-2-oleoylphosphatidylserine (SOPS) either with or without cholesterol in the form of multilamellar vesicles. The SOPC is similar to forms of phosphatidylcholine that occur in cell membranes; as a pure lipid, it has a melting temperature of 6 °C, while that of SOPS is 17 °C. The DPPC has a melting temperature at 42 °C, similar to that of sphingomyelin. The samples were subjected to three cycles of freezing and thawing. In the case of mixtures with DPPC, a lipid with a phase transition temperature of 42 °C, the samples were heated to 45 °C after each freezing. All lipid/protein mixtures, as well as the controls, were then incubated for 30 min at 37 °C.

Centrifugation Assay for Membrane Binding of NAP-22. Membrane binding of NAP-22 was assessed by modification of the previously described procedure (*12*), except that the lipid was in the form of MLV instead of sonicated vesicles. The DOPC mixed with 40 mol % cholesterol was codissolved in a 2/1 chloroform/methanol mixture and the lipid deposited on the walls of a glass test tube by solvent evaporation with a stream of nitrogen gas. The last traces of solvent were then removed by evaporation for 2 h under vacuum. To this lipid film was added a solution of NAP-22 in 10 mM Tris-HCl, 150 mM NaCl, 2 mM $MgCl_2$, 0.2 mM EGTA, and 1 mM dithiothreitol (pH 7.5) to give the desired final lipid-to-protein ratio. The lipid was suspended by vortexing the mixture at room temperature followed by three cycles of freezing and thawing. All lipid/protein mixtures, as well as the controls, were then incubated for 30 min at 37 °C. The vesicles with bound protein were then pelleted by centrifugation at 200000*g* for 90 min at 25 °C. The supernatant was removed and assayed for protein and lipid.

Determination of Phospholipid Concentrations. The concentration of phospholipid was determined by measuring the amount of inorganic phosphate released after digestion by the method of Ames (*22*).

Determination of the Protein Concentrations. The concentration of NAP-22 was determined by either the BCA assay (Pierce Chemical Co.) or the CBQCA assay (Molecular Probes). In addition, the protein was identified by SDS−PAGE after staining with Coomasie Blue.

Detergent Resistant Membranes. NAP-22 was incorporated into MLV of DPPC with 40% cholesterol {containing 0.05 μCi of [7-^{3}H(N)]cholesterol} by freezing and thawing three times, as described above. The final lipid concentration was 3.2 mM, and the lipid-to-protein ratio was 200. A lipid control without NAP-22 was run in parallel. The suspension was cooled in an ice bath, and an equal volume of ice-cold 2% Triton X-100 was added to give a final Triton concentration of 1%. The mixture was then kept on ice for 30 min and then centrifuged at 4 °C and 200000*g* for 90 min. The pellet and supernate fractions were separated, and the amount of [^{3}H]cholesterol in each fraction was determined by scintillation counting after correcting for quenching by Triton. Phospholipid concentrations were determined in the pellet by phosphate analysis (*22*), and the protein concentration was determined in the supernatant as described above.

Differential Scanning Calorimetry (DSC). Multilamellar suspensions of phospholipid at a concentration of 2.3 mg/mL were prepared by hydrating dry lipid films with either pure buffer or a solution of NAP-22 as described above to give a final lipid-to-protein ratio of 500. The buffer that was used included 10 mM Tris-HCl, 150 mM NaCl, 2 mM $MgCl_2$, 0.2 mM EGTA, and 1 mM dithiothreitol (pH 7.5). Suspensions were degassed under vacuum before being loaded into a NanoCal high-sensitivity calorimeter (CSC, Spanish Forks, UT). Both heating and cooling DSC scans were run at a rate of 0.75 °C/min. The observed phase transition was fitted, using Origin 5.0, with parameters describing an equilibrium with a single van't Hoff enthalpy.

Preparation of Samples for AFM. DOPC and 0.4 mole fraction cholesterol were combined in a solution of chloroform and methanol (2/1, v/v). The lipids were deposited on the walls of a glass test tube by solvent evaporation under a stream of nitrogen. The last traces of solvent were removed under vacuum for 2 h. The film was hydrated with 10 mM sodium phosphate buffer and 0.15 M NaCl (pH 7.4) to give a final lipid suspension of 1 mg/mL. This suspension was then placed in a bath type sonicator for approximately 20 min, until the suspension became clear or only slightly hazy.

[1] Abbreviations: DSC, differential scanning calorimetry; MLV, multilamellar vesicles; AFM, atomic force microscopy; TMAFM, tapping mode AFM; DOPC, dioleoylphosphatidylcholine; SOPC, 1-stearoyl-2-oleoylphosphatidylcholine; DPPC, dipalmitoylphosphatidylcholine; SOPS, 1-stearoyl-2-oleoylphosphatidylserine.

This lipid suspension was then applied to the surface of freshly cleaved mica and the lipid allowed to adhere to the mica surface over a period of 10−20 min.

Atomic Force Microscopy. Solution tapping mode atomic force microscopy (TMAFM) images were acquired on a Digital Instruments Nanoscope IIIA MultiMode scanning probe microscope (Digital Instruments, Santa Barbara, CA) using 120 μm oxide-sharpened silicon nitride V-shaped cantilevers installed in a combination contact/tapping mode liquid flow cell. The flow cell was fitted with inlet and outlet tubes to enable direct fluid exchange during imaging. The AFM cantilevers were irradiated with UV light prior to imaging to remove any adventitious organic contaminants. The AFM images were acquired using the E scanning head, which has a maximum lateral scan area of 14.6 μm × 14.6 μm. All imaging was performed at tip scan rates from 1.25 to 2 Hz, using cantilever drive frequencies of ~8.9 kHz at ambient temperature. All images were captured as 512 × 512 pixel images and were low-pass filtered. Feature size and volumes were calculated using the Digital Instruments Nanoscope software (version 4.21) and a shareware image analysis program, NIH Image (version 1.62). Supported bilayers were formed by directly injecting ~500 μL of the 1 mg/mL lipid suspension into the AFM fluid cell, previously sealed against a piece of freshly cleaved mica, and allowing the vesicles to fuse in situ. The cell was flushed with buffer, and reference TMAFM height and phase images were acquired in protein-free 10 mM sodium phosphate, 150 mM NaCl buffer at pH 7.4 to confirm formation of a stable lipid bilayer. Approximately 500 μL of the protein solution in the same buffer was added and the sample imaged again to obtain reference images of the membrane-associated proteins. Since the AFM fluid cell volume is ~200 μL, we have ensured complete replacement of the original imaging buffer. At no time was the AFM cell removed from the mica surface, nor was the lipid bilayer exposed to air.

RESULTS

Circular Dichroism (CD). Little is known about the conformational properties of NAP-22. The protein has been shown to be resistant to denaturation (*16*). Secondary structure predictions suggest that NAP-22 could contain a significant amount of α-helical character (*16*). We have therefore undertaken a CD study to characterize the secondary structure of NAP-22 and to assess how sensitive this structure is to variations in pH and buffer conditions as well as to the presence of liposomes.

Under a variety of conditions, NAP-22 has very little α-helical structure (Table 1). Even the addition of 65% trifluoroethanol, a solvent that is very potent in inducing helical structure, had only a very modest effect on either the CD spectrum (Figure 1) or the calculated secondary structure (Table 1). However, the CD results do indicate that NAP-22 does contain significant amounts of β-structure (Table 1). Although estimates of β-structure content by CD are not very accurate, our results strongly suggest that NAP-22 is essentially devoid of α-helical structure but has a significant β-structure content.

The secondary structure, as determined by CD spectroscopy, is not sensitive to changes in conditions in aqueous solution as evidenced by the lack of significant variations in the CD spectra as the solution pH was varied from 7.4 to 4.5, the latter pH being close to the isoelectric point of NAP-22. The addition of sonicated liposomes of SOPC or of SOPS containing 0.4 mole fraction cholesterol also did not promote any significant secondary structure changes (Table 1). The minor changes are likely a consequence of light scattering effects.

Table 1: Secondary Structure of 15 μM NAP-22 at 37 °C

condition	secondary structure (fraction of total)[a]		
	α-helix	β-structure	random
buffer[b]	0.07 (0)	0.51 (0.47)	0.42 (0.53)
65% TFE/buffer	0.08 (0.08)	0.41 (0.16)	0.51 (0.76)
0.5 mM SOPC and 0.4 mole fraction cholesterol	ND (0)	ND (0.30)	ND (0.70)
0.5 mM SOPS and 0.4 mole fraction cholesterol[c]	ND (0)	ND (0.36)	ND (0.64)

[a] Values are given for analysis by a neural network program (*39*), followed by an estimate given in parentheses that was obtained by analysis of the same data using the curve fitting procedure of Yang et al. (*40*). ND indicates that the method was not able to estimate the value within a reasonable uncertainty. [b] Includes 10 mM sodium phosphate, 0.14 M NaF, and 1 mM EDTA (pH 7.4). [c] The protein-to-lipid molar ratio was 1/500.

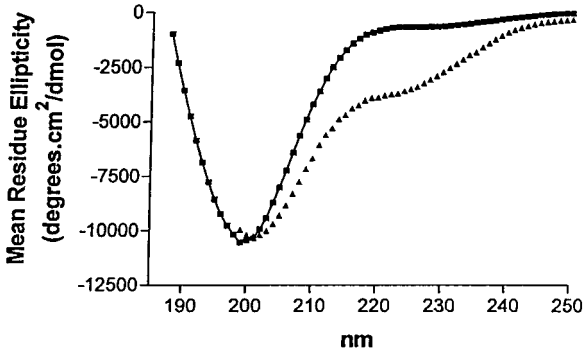

FIGURE 1: Circular dichroism spectra of 15 μM NAP-22 in 10 mM sodium phosphate, 140 mM NaF, and 1 mM EDTA (pH 7.4) (■) and diluted with TFE to 65% TFE (▲).

Membrane Binding. The lipid dependence of NAP-22 binding to small sonicated vesicles has already been reported by Maekawa (*12*). Since sonicated vesicles are strained, we have repeated and extended these results using MLV, separating membrane-bound and free protein by centrifugation. In the absence of cholesterol, none of the three forms of phosphatidylcholine (DPPC, DOPC, or SOPC) nor SOPS extracted significant amounts of NAP-22 from the supernatant into the pellet fraction, in agreement with the results reported earlier with PC and with PS membranes (*12*). With 0.4 mole fraction cholesterol and either SOPC, DOPC, or DPPC, the major fraction of NAP-22 did transfer to the membrane. In the case of DPPC, the samples were heated to 45 °C after each freeze−thaw cycle so that the lipid would be in the L_α phase. The dependence of the partitioning of NAP-22 to MLV on the SOPC/cholesterol ratio (data not presented) was similar to that previously observed using sonicated vesicles (*12*). The results presented here confirm the findings of Maekawa and further demonstrate that the binding of NAP-22 to cholesterol-containing membranes does not require the high curvature strain of sonicated vesicles. In addition, we have found that NAP-22 partitioning is insensitive to the fatty acid composition of the phospha-

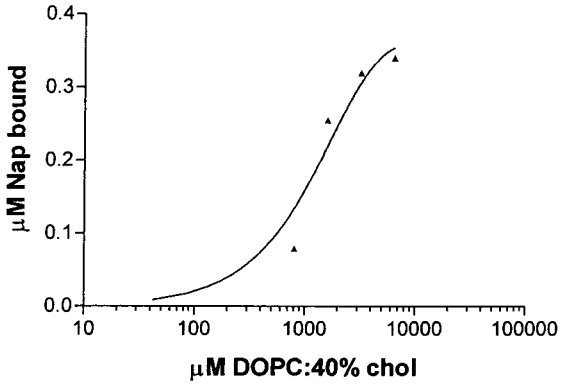

FIGURE 2: Binding of NAP-22 to membranes of DOPC with 40% cholesterol.

tidylcholine. However, in contrast to the acyl chains, changing the headgroup from zwitterionic phosphatidylcholine to anionic phosphatidylserine virtually completely eliminated binding to lipid even in the presence of an equimolar amount of cholesterol, in agreement with the previously published findings (*12*).

We have also measured the affinity of binding of NAP-22 to membranes of DOPC with 40% cholesterol (Figure 2). The binding curve was analyzed to obtain a partition coefficient (*23*, *24*), and the free energy of NAP-22 binding to this membrane was calculated to be -7.3 ± 0.5 kcal/mol of protein.

Triton Solubilization. In the absence of protein, the DPPC with 40% cholesterol forms, as expected, a detergent insoluble material. In this pellet, we find only 40% of the total initial amount of cholesterol (Figure 3). This is somewhat smaller than that found by Schroeder et al. (*25*); however, in that work, a lower ratio of Triton to lipid was used (personal communication), and their lipid was in a different physical form as detergent-dialyzed large unilamellar vesicles. Addition of NAP-22 at a protein to lipid molar ratio of 1/200 increases the amount of cholesterol in the pellet but decreases the amount of phospholipid in the pellet. The cholesterol was assayed in both pellet and supernate fractions, but the DPPC was assayed only in the pellet fraction because of interference by Triton in the phosphate assay. The protein was assayed only on the supernatant because of interference by lipid in the protein assay.

Effect of NAP-22 on Lipid Phase Behavior. We employed differential scanning calorimetry (DSC) to monitor lipid phase transitions both in the presence and in the absence of NAP-22. At a protein to lipid molar ratio of 1/500, NAP-22 was found to have no effect on the temperature, enthalpy, or cooperativity of the L_α to L_β phase transition of DPPC in the absence of cholesterol (Table 2). Since the chain melting transition of DPPC at 42 °C is sharp and of high enthalpy, even a minor change in the transition characteristics could have been detected by the calorimetric analysis. Remarkably, even the $P_{\beta'}$ to L_α phase transition of DPPC, which occurs at 36 °C and is known to be very sensitive to the presence of additives in the membrane, is hardly affected by the presence of NAP-22 (Table 2). However, NAP-22 has a significant effect on the L_β to L_α phase transition when a phosphatidylcholine was mixed with cholesterol. It is known that even in the absence of protein, mixtures of both DPPC

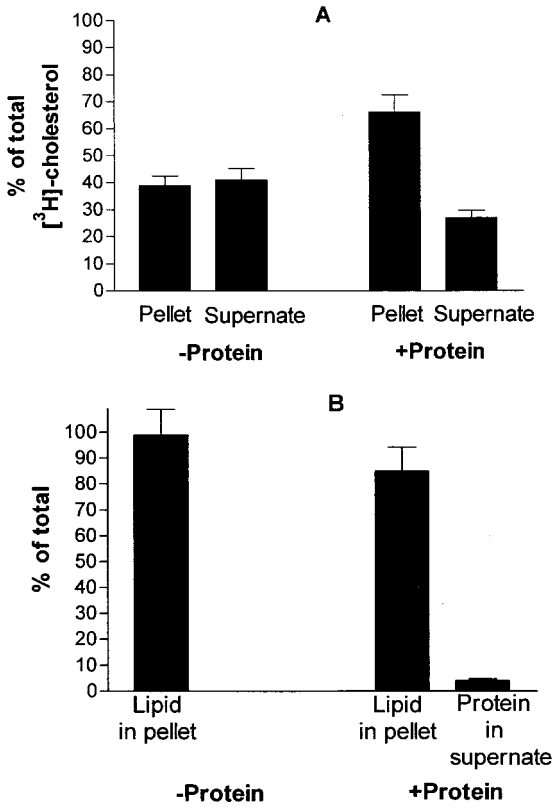

FIGURE 3: Triton solubility of a mixture of DPPC and 40% cholesterol with and without NAP-22. (A) Percent of total cholesterol in the Triton insoluble pellet vs the Triton soluble supernate without (left) or with (right) NAP-22. (B) Percent of total lipid in the Triton insoluble pellet without (left) or with (right) NAP-22 and percent of total protein in the Triton soluble supernate (right). The lipid to protein molar ratio is 200/1.

Table 2: Calorimetric Heating Transitions

	NAP-22[a]	T_M (°C)	component	ΔH_{cal} (kcal)	total ΔH_{cal} (kcal)
DPPC	no	42.2		5.6	5.6
DPPC	yes	42.1		5.4	5.4
DPPC	no	36.0		0.8	0.8
DPPC	yes	35.8	1	0.7	
DPPC	yes	33.1	2	0.1	0.8
DPPC and 0.3 chol[b]	no	41.4		0.14	0.14
DPPC and 0.3 chol	yes	41.3	1	0.15	
DPPC and 0.3 chol	yes	41.9	2	0.08	0.23
DPPC and 0.4 chol	no	40.5	1	0.12	
DPPC and 0.4 chol	no	41.6	2	0.10	0.22
DPPC and 0.4 chol	yes	40.5	1	0.19	
DPPC and 0.4 chol	yes	42.1	2	0.11	0.30
DPPC and 0.4 chol	yes	95.2		0.05	0.05
SOPC and 0.4 chol	no	6.0		0.3	0.3
SOPC and 0.4 chol	yes	3.5	1	0.01	
SOPC and 0.4 chol	yes	5.5	2	0.04	
SOPC and 0.4 chol	yes	7.0	3	0.02	0.07
SOPC and 0.4 chol	yes	36.8		0.03	0.03
SOPC and 0.4 chol	yes	95.0		0.01	0.01

[a] When present, the NAP-22-to-lipid molar ratio is 1/500. [b] Cholesterol (chol) given as mole fraction.

(*26*) and SOPC (*27*) with cholesterol exhibit both a sharp and a broad component for the L_β to L_α phase transition. The transition enthalpy of mixtures of a phosphatidylcholine with cholesterol is much lower than that of the same phospholipid in pure form. There is also a still broader component that would require higher concentrations to be

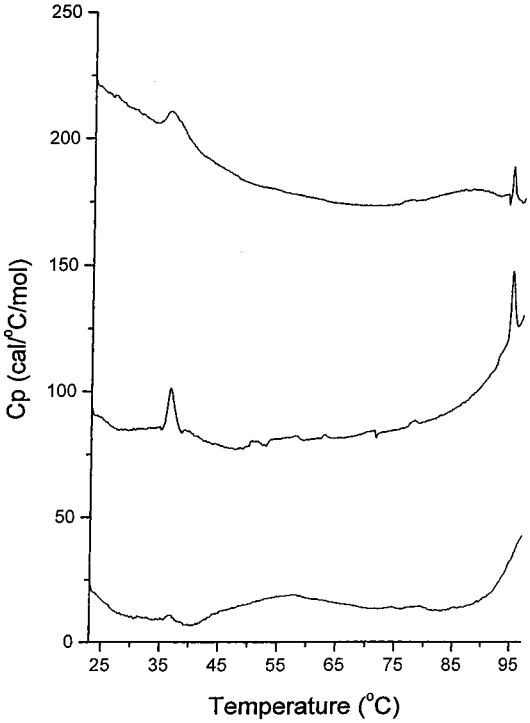

FIGURE 4: Heating scans of SOPC with 0.4 mole fraction cholesterol at a scan rate of 0.75 °C/min showing cholesterol crystallite transitions. This plot was expanded to show the low-enthalpy, broad peaks of the phospholipid transition. The bottom curve is a control for SOPC with 0.4 mole fraction cholesterol. The middle curve is the first heating scan of SOPC in the presence of NAP-22 at a protein-to-lipid ratio of 1/500. The top curve is the second heating scan of the same sample of SOPC with NAP-22.

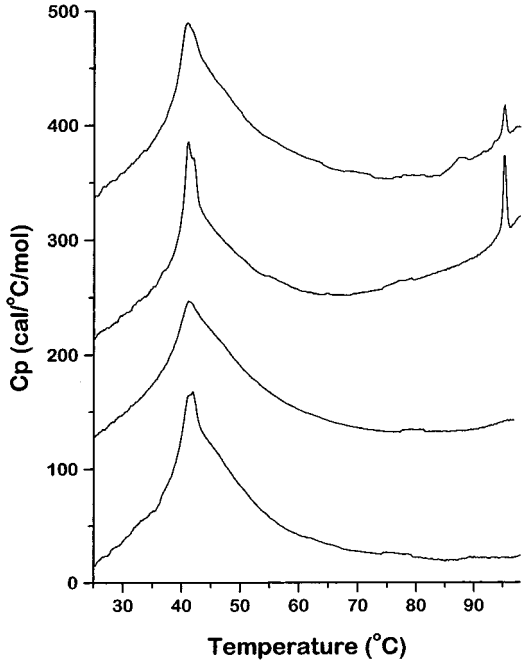

FIGURE 5: Heating scans of DPPC with 0.4 mole fraction cholesterol at a scan rate of 0.75 °C/min showing a cholesterol crystallite transition at 95 °C. Top two curves are in the presence of NAP-22 at a protein-to-lipid ratio of 1/500 with the next to the top curve being the first scan and the top curve being the second heating scan. The bottom two curves are with the same lipid composition but without protein, with the first scan being the one on the bottom.

observed accurately. Since large amounts of protein were not available, this aspect was not investigated.

Addition of NAP-22 to DPPC with 0.3 mole fraction cholesterol results in the observable sharper component being split into two components. One of the components observed upon the addition of protein has a transition temperature close to that of the pure DPPC in the absence of cholesterol (Table 2). This suggests that NAP-22 can sequester cholesterol into domains in the membrane, leaving other regions largely devoid of this lipid. A similar splitting of the main transition is observed with SOPC containing 0.4 mole fraction cholesterol (Table 2). The fact that NAP-22 can significantly increase the enthalpy of the observed transition (Table 2), and split it into two peaks, one of which is coincident with the phase transition temperature of the pure phospholipid, indicates that the protein is depleting a region of the membrane from cholesterol. The NAP-22 thus induces the formation of a phospholipid-rich region which has a higher enthalpy and altered phase transition temperature. Since the amount of cholesterol does not change, this must also mean that cholesterol-enriched domains are forming in the membrane.

The sequestering of cholesterol into domains in the membrane is further demonstrated by appearance of peaks corresponding to phase transitions of cholesterol "crystallites" (Figures 4 and 5). These peaks appear in PC/cholesterol samples containing NAP-22, but not in pure lipid samples of the same lipid composition. It is known that anhydrous cholesterol undergoes a polymorphic transition at ~38 °C (*28*). In cooling scans, this transition undergoes a marked undercooling, and at the scan rate used here, 0.75 °C/min, the transition occurs at ~19 °C (*29*). These same transitions, corresponding to the polymorphic transition of anhydrous cholesterol, were observed with the samples of SOPC containing 0.4 (Figure 4) or 0.5 (not shown) mole fraction cholesterol but only in the presence of NAP-22. In the absence of this protein, no cholesterol crystallites have ever been observed for phosphatidylcholine mixtures having ≤0.5 mole fraction cholesterol.

There was no effect of NAP-22, at a similar 1/500 molar ratio, on the phase transition properties of SOPS containing 0.3 mole fraction cholesterol. This is consistent with the lack of binding of NAP-22 to these membranes. Higher cholesterol concentrations were not used since we have shown that, even at 0.4 mole fraction cholesterol, there is a considerable amount of cholesterol crystallites found in pure lipid samples with SOPS without NAP-22 (*29*). Thus, although cholesterol crystallites form more readily in SOPS than in SOPC, NAP-22 promotes the formation of these "crystallites" specifically in SOPC.

AFM. In situ AFM imaging revealed the gradual formation of a molecularly smooth bilayer by direct fusion of sonicated DOPC vesicles containing 0.4 mole fraction cholesterol to freshly cleaved mica. Removal of the deposited bilayer from a small region allowed measurement of the thickness of the deposit. The thickness of the bilayer, measured from an exposed mica surface, not immediately surrounding the exposed mica, is 5.4 ± 0.2 nm (Figure 6A). While these bilayer heights are somewhat greater than the 4.5 nm measured for DOPC bilayers by diffraction (*30*, *31*), water between the bilayer and the supporting mica may account for this difference (*32*).

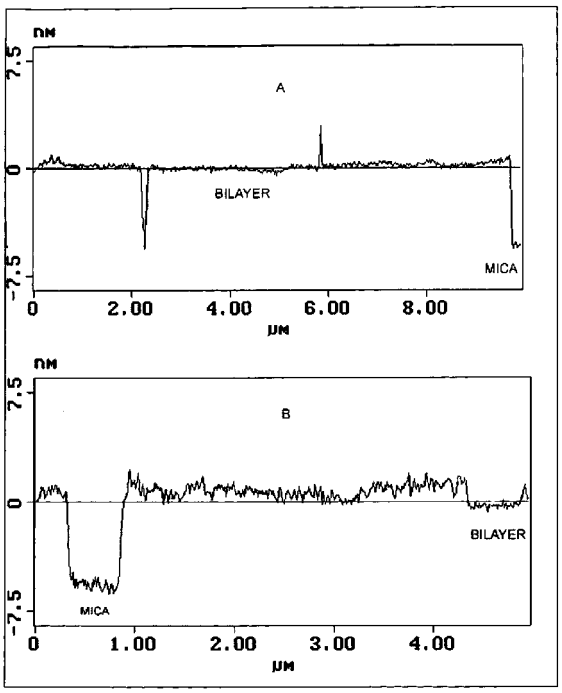

FIGURE 6: Examples of height measurement in regions of the specimen in which a small region of bare mica appears. (A) DOPC with 0.4 mole fraction cholesterol in the absence of protein. (B) Same lipid after the addition of NAP-22.

In situ imaging performed immediately after the addition of an aliquot of the NAP-22 protein revealed a dramatic change in the surface topography of the bilayer (Figure 7). As can be seen in the gray-scale encoded height images, extended duration in situ imaging revealed the gradual expansion of micrometer-sized dendritic domains extending ~1.5 nm above the underlying bilayer (Figure 6B) over the span of several hours (Figure 7). These regions did not appear molecularly smooth (Figure 8).

DISCUSSION

Proteins that insert into membranes acquire a high content of secondary structure, most often α-helical. The fact that NAP-22 does not have a higher content of secondary structure in the presence of liposomes indicates that this protein does not insert deeply into the bilayer. This is in agreement with the binding energy of −7.3 kcal/mol that we find for NAP-22 binding to liposomes of DOPC with 40% cholesterol. This is comparable to the value of −8 kcal/mol found by Peitzsch and McLaughlin (*24*) for the binding of a myristoyl group to a membrane. Thus, the energy of interaction between the protein and membrane is largely accounted for by the insertion of the myristoyl group into the membrane. The protein portion of NAP-22 does not have a high affinity for these membranes.

Nevertheless, NAP-22 does exhibit lipid specificity for binding to membranes and will only bind to liposomes containing cholesterol. A property that is frequently used to identify raft components of cholesterol-rich regions in membranes is their detergent insolubility. By this criterion, NAP-22 is a typical raft protein, since it essentially completely partitions into the detergent insoluble fraction (Figure 3). Interestingly, NAP-22 also causes the cholesterol-to-phospholipid ratio to increase in the detergent insoluble pellet, compared with the protein-free control. This may help to explain the high fraction of cholesterol found in the detergent insoluble fraction of neuronal membranes that is enriched in NAP-22 (*12*). NAP-22 is known to be myristoylated (*19*), and such lipidation has been shown to be sufficient to cause proteins to partition into detergent insoluble domains (*13*). It has been suggested that high-melting sphingolipids or phospholipids promote the sequestering of cholesterol into rafts because of favorable interactions between saturated acyl chains and cholesterol (*5*). The lipid in these domains is in the liquid ordered phase. However, at high cholesterol mole fractions, the physical state of the membrane with phosphatidylcholine having saturated acyl chains may not be very different from those containing low-melting, unsaturated acyl chains (*33*), even though the mixtures with unsaturated acyl chains are not detergent insoluble (*25*). Thus, although neuronal rafts appear not to have a high mole fraction of sphingomyelin, their physical state may not be very different from that of the sphingomyelin-rich rafts and caveoli. However, the driving force for the formation of the neuronal rafts appears to be quite different, being dependent on the interaction of proteins such as NAP-22 with cholesterol, while for the more common types of rafts, the phase behavior of the lipid components alone appears to be sufficient to explain the formation of these domains (*34*).

We demonstrate by a variety of methods that NAP-22 is capable of enriching membrane domains with cholesterol, including the formation of cholesterol aggregates that give rise to calorimetric transitions. Pure anhydrous cholesterol exhibits a polymorphic transition at ~38 °C, and in excess water, these crystals slowly transform, over a period of many hours, to crystals of cholesterol monohydrate that normally

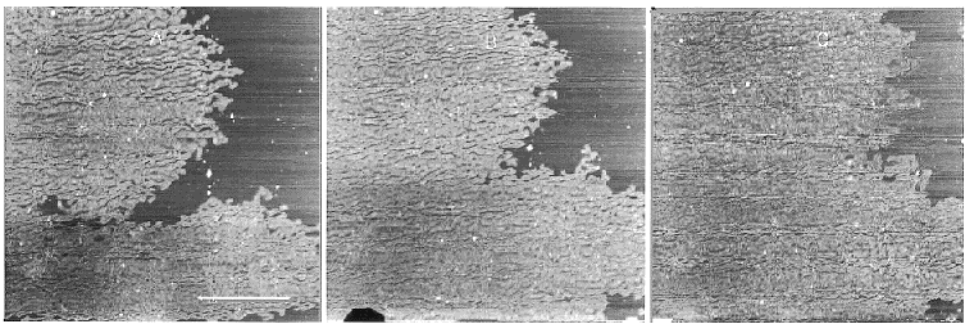

FIGURE 7: AFM height images of DOPC with 0.4 mole fraction cholesterol in the presence of NAP-22 taken 10 (A), 15 (B), and 20 min (C) after the addition of protein. The calibration bar shown in panel A represents 1.24 μm and is the same for all three images (full size, 5 μm × 5 μm). These images were taken over the same region of the specimen for the various time points.

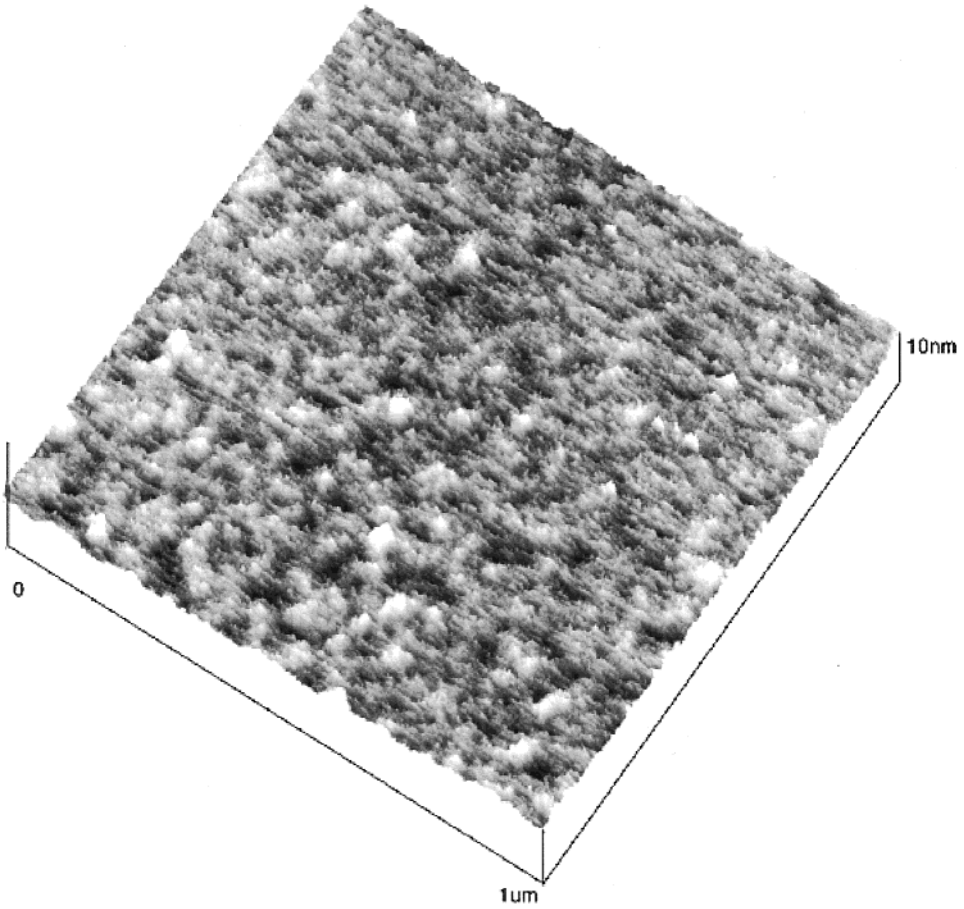

FIGURE 8: Three-dimensional topology of DOPC with 0.4 mole fraction cholesterol in the presence of NAP-22 in a domain showing rough surface contour.

undergoes a dehydration transition at ~80 °C (*28*). Only in the presence of anionic lipids, such as phosphatidylserine (*29*), does cholesterol forms crystallites at mole fractions of ≤0.5. We have recently shown that, in membranes of phosphatidylserine and cholesterol, the dehydration transition is shifted to 95 °C after incubation of aqueous suspensions of the sample for several days, but never in fresh samples (*35*). Corresponding to the dehydration of cholesterol, this same transition is observed in freshly prepared SOPC/cholesterol (Figure 4) and DPPC/cholesterol mixtures (Figure 5) when NAP-22 was present. Furthermore, unlike the irreversible dehydration that occurs at 80 °C, we find that the 95 °C transition, both with a phosphatidylserine/cholesterol mixture after incubation (without protein) and with a SOPC/cholesterol mixture in the presence of NAP-22, is partially reversible on reheating (Figures 4 and 5). A transition at this temperature has never been observed with membranes of phosphatidylcholine and cholesterol in the absence of protein and is only seen with phosphatidylserine/cholesterol mixtures after many days of incubation (*35*). Our observations of this transition in fresh samples of phosphatidylcholine and cholesterol in the presence of NAP-22 are strong evidence that the protein is affecting the reorganization of cholesterol in the membrane. We believe that due to the high solubility of cholesterol in phosphatidylcholine membranes, it is unlikely that cholesterol is forming a crystal of macroscopic dimensions. Rather, these crystallites may represent clusters of cholesterol molecules within the membrane. In addition to promoting the formation of cholesterol crystallites, NAP-22 increases the enthalpy of the phospholipid chain melting transition and it induces the formation of a cholesterol-depleted domain having a sharp phase transition at the temperature corresponding to that of the pure phospholipid. These phenomena occur to a detectable extent at a relatively low protein to lipid molar ratio of 1/500, and they do not require sphingomyelin or saturated forms of phosphatidylcholine.

Atomic force microscopy provided dramatic evidence of the ability of NAP-22 to initiate domain formation. This approach has been used by others to characterize lipid domain structures (*36*, *37*). Addition of the protein to a supported bilayer of DOPC and 0.4 mole fraction cholesterol led to the rapid formation of an irregularly shaped ~1 nm thick overlayer on the supporting lipid bilayer (Figure 7). We attribute this effect to direct deposition of NAP-22 onto the surface of the bilayer as a consequence of binding (Figure 8). Since the overlayer thickness is smaller than the calculated model diameter (3.7 nm) of NAP-22, modeled as a 22 kDa globular protein, this would suggest that the NAP-22 molecule either is partially embedded into the supporting lipid bilayer or has adopted an anisotropic orientation, which is consistent with our CD data indicating a high degree of β-structure.

X-ray diffraction studies have shown that the addition of an equimolar concentration of cholesterol to egg phosphatidylcholine bilayers results in a small 0.2 nm increase in thickness (*38*). This difference is within the error of AFM using different samples, i.e., comparing the thickness of the

pure lipid bilayer with that of the smooth region of the bilayer in the presence of NAP-22. We therefore cannot conclude from our AFM measurements whether these smooth regions devoid of an overlayer, which are observed in the presence of NAP-22, are depleted of cholesterol. However, AFM does show the different texture of the protein-rich regions and illustrates that these regions are spatially segregated in the membrane and that the protein does not protrude very far from the surface of the membrane.

The lack of binding of NAP-22 to membranes of PS may be a consequence of the protein having an overall negative charge at neutral pH and therefore not binding to anionic lipid. However, NAP-22 has a cluster of cationic residues near the amino terminus, and it has been suggested that NAP-22 binds to the anionic lipid, phosphatidylinositol diphosphate (*15*). Furthermore, NAP-22 is a substrate for protein kinase C, an enzyme requiring a cluster of cationic residues for specificity. It is possible that the affinity of NAP-22 for a DOPC/cholesterol mixture will increase when low mole fractions of PS are added to the membrane (work in progress).

This work demonstrates that when NAP-22 binds specifically to membranes containing a high mole fraction of cholesterol, it promotes the formation of cholesterol-rich domains in these membranes. This could be of relevance in the mechanism by which these domains form at the neuronal growth cone in the developing brain. Furthermore, AFM shows very directly that NAP-22 induces the formation of domains when it binds to the surface of membrane bilayers.

REFERENCES

1. Janes, P. W., Ley, S. C., Magee, A. I., and Kabouridis, P. S. (2000) *Semin. Immunol. 12*, 23−34.
2. Simons, K., and Toomre, D. (2000) *Nat. Rev.: Mol. Cell Biol. 1*, 31−39.
3. Langlet, C., Bernard, A. M., Drevot, P., and He, H. T. (2000) *Curr. Opin. Immunol. 12*, 250−255.
4. Ge, M., Field, K. A., Aneja, R., Holowka, D., Baird, B., and Freed, J. H. (1999) *Biophys. J. 77*, 925−933.
5. Brown, D. A., and London, E. (2000) *J. Biol. Chem. 275*, 17221−17224.
6. Ostermeyer, A. G., Beckrich, B. T., Ivarson, K. A., Grove, K. E., and Brown, D. A. (1999) *J. Biol. Chem. 274*, 34459−34466.
7. Kenworthy, A. K., Petranova, N., and Edidin, M. (2000) *Mol. Biol. Cell 11*, 1645−1655.
8. Schutz, G. J., Kada, G., Pastushenko, V. P., and Schindler, H. (2000) *EMBO J. 19*, 892−901.
9. Pralle, A., Keller, P., Florin, E. L., Simons, K., and Horber, J. K. (2000) *J. Cell Biol. 148*, 997−1008.
10. Edidin, M. (1997) *Curr. Opin. Struct. Biol. 7*, 528−532.
11. Iino, S., Kobayashi, S., and Maekawa, S. (1999) *Neuroscience 91*, 1435−1444.
12. Maekawa, S., Sato, C., Kitajima, K., Funatsu, N., Kumanogoh, H., and Sokawa, Y. (1999) *J. Biol. Chem. 274*, 21369−21374.
13. Moffett, S., Brown, D. A., and Linder, M. E. (2000) *J. Biol. Chem. 275*, 2191−2198.
14. Widmer, F., and Caroni, P. (1990) *J. Cell Biol. 111*, 3035−3047.
15. Laux, T., Fukami, K., Thelen, M., Golub, T., Frey, D., and Caroni, P. (2000) *J. Cell Biol. 149*, 1455−1472.
16. Maekawa, S., Maekawa, M., Hattori, S., and Nakamura, S. (1993) *J. Biol. Chem. 268*, 13703−13709.
17. Frey, D., Laux, T., Xu, L., Schneider, C., and Caroni, P. (2000) *J. Cell Biol. 149*, 1443−1454.
18. Bomze, H. M., Bulsara, K. R., Iskandar, B. J., Caroni, P., and Pate Skene, J. H. (2001) *Nat. Neurosci. 4*, 38−43.
19. Takasaki, A., Hayashi, N., Matsubara, M., Yamauchi, E., and Taniguchi, H. (1999) *J. Biol. Chem. 274*, 11848−11853.
20. Andrade, M. A., Chacon, P., Merelo, J. J., and Moran, F. (1993) *Protein Eng. 6*, 383−390.
21. Chang, C. T., Wu, C. S., and Yang, J. T. (1978) *Anal. Biochem. 91*, 13−31.
22. Ames, B. N. (1966) *Methods Enzymol. 8*, 115−118.
23. Kim, J., Blackshear, P. J., Johnson, J. D., and McLaughlin, S. (1994) *Biophys. J. 67*, 227−237.
24. Peitzsch, R. M., and McLaughlin, S. (1993) *Biochemistry 32*, 10436−10443.
25. Schroeder, R., London, E., and Brown, D. (1994) *Proc. Natl. Acad. Sci. U.S.A. 91*, 12130−12134.
26. McMullen, T. P., and McElhaney, R. N. (1995) *Biochim. Biophys. Acta 1234*, 90−98.
27. Vilcheze, C., McMullen, T. P., McElhaney, R. N., and Bittman, R. (1996) *Biochim. Biophys. Acta 1279*, 235−242.
28. Loomis, C. R., Shipley, G. G., and Small, D. M. (1979) *J. Lipid Res. 20*, 525−535.
29. Epand, R. M., Bach, D., Borochov, N., and Wachtel, E. (2000) *Biophys. J. 78*, 866−873.
30. Tristram-Nagle, S., Petrache, H. I., and Nagle, J. F. (1998) *Biophys. J. 75*, 917−925.
31. Costigan, S. C., Booth, P. J., and Templer, R. H. (2000) *Biochim. Biophys. Acta 1468*, 41−54.
32. Tamm, L., and Shao, Z. (1998) in *Biomembrane Structures* (Harris, P. I., and Chapman, D., Eds.) pp 169−185, IOS Press, Amsterdam.
33. Mateo, C. R., Ulises, A. A., and Brochon, J. C. (1995) *Biophys. J. 68*, 978−987.
34. Estep, T. N., Freire, E., Anthony, F., Barenholz, Y., Biltonen, R. L., and Thompson, T. E. (1981) *Biochemistry 20*, 7115−7118.
35. Epand, R. M., Bach, D., Epand, R. F., Borochov, N., and Wachtel, E. (2001) *Biophys. J. 81*, 1511−1520.
36. Hollars, C. W., and Dunn, R. C. (1998) *Biophys. J. 75*, 342−353.
37. McKiernan, A. E., Ratto, T. V., and Longo, M. L. (2000) *Biophys. J. 79*, 2605−2615.
38. McIntosh, T. J., Magid, A. D., and Simon, S. A. (1989) *Biochemistry 28*, 17−25.
39. Andrade, M. A., Chacon, P., Merelo, J. J., and Moran, F. (1993) *Protein Eng. 6*, 383−390.
40. Chang, C. T., Wu, C. S., and Yang, J. T. (1978) *Anal. Biochem. 91*, 13−31.

BI010897S